ELSEVIER

International Journal of Pharmaceutics 217 (2001) 173–181

international journal of pharmaceutics

www.elsevier.com/locate/ijpharm

Quantitative determination of the specific heat and the glass transition of moist samples by temperature modulated differential scanning calorimetry

Markus Schubnell *, Jürgen E.K. Schawe

Mettler Toledo GmbH, Sonnenbergstrasse 74, CH-8603 Schwerzenbach, Switzerland

Received 18 May 2000; received in revised form 14 December 2000; accepted 27 January 2001

Abstract

In differential scanning calorimetry (DSC), remnant moisture loss in samples often overlaps and distorts other thermal events, e.g. glass transitions. To separate such overlapping processes, temperature modulated DSC (TMDSC) has been widely used. In this contribution we discuss the quantitative determination of the heat capacity of a moist sample from TMDSC measurements. The sample was a spray-dried pharmaceutical compound run in different pans (hermetically-sealed pan, pierced lid pan [50 μm] and open pan). The apparent heat capacity was corrected for the remaining amount of moisture. Using this procedure we could clearly identify the glass transition of the dry and the moist sample. We found that a moisture content of about 6.2% shifts the glass transition by about 50°C.

Keywords: Temperature modulated DSC; Specific heat; Glass transition; Moisture

1. Introduction

Samples that have to be analyzed by differential scanning calorimetry (DSC) often contain some moisture (or, more generally, some volatile solvent) remnant from the production process (e.g. spray-drying). Typical examples of such samples are pharmaceutical compounds or applications from the food industry. In a conventional DSC experiment, such samples typically show a broad endothermic peak due to the evaporation of the water still present. The evaporation signal usually dominates any other processes that might be present. Because moisture can influence other thermal effects (e.g. it may act as a plastiziser thus shifting the glass transition) the measurements of a dry sample (second run) could deliver different results. Therefore, moist samples are generally well suited for a temperature modulated DSC (TMDSC) analysis. In TMDSC a sinusoidal temperature modulation is superimposed onto a conventional linear temperature program, leading to a modulated heat flow. This technique has been frequently used to separate overlapping thermal

* Corresponding author. Tel: +41-1-806-7408; fax: +41-1-806-7350.

E-mail address: markus.schubnell@mt.com (M. Schubnell).

0378-5173/01/$ - see front matter
PII: S0378-5173(01)00601-9

effects, e.g. cold crystallization and glass transition of polymer blends (Jin et al., 1996; Cheng et al., 1997); the measurement of the heat capacity during crystallization or curing reactions (Cassettari et al., 1992; Reading, 1993; Schawe & Höhne, 1996; Toda et al., 1997; Van Assche et al., 1997; Monserrat & Cima, 1999); phase separation during reactions (Alig et al., 1998; Swier & Van Mele, 1999); and moisture loss and glass transitions (Sichina, 1994; Riesen et al., 1996; Royall et al., 1999; Hill et al., 1998). It is well known that for semi-crystalline non-polymeric materials, the step height of the specific heat capacity in the glass transition region is proportional to the content of the amorphous phase (Schick et al., 1991). This has been used by Guinot & Leveiller (1999) to determine the crystallinity of drugs by TMDSC. A method for investigating the influence of moisture on the glass transition temperature of amorphous drugs is presented by Royall et al. (1999).

If the sample is prepared in a non-hermetically-sealed DSC-pan, an endothermic evaporation peak is superimposed onto the proper sample transitions. Additionally, the change in moisture could influence the glass transition region of the drugs as well. In this paper we show, for an example of a moist pharmaceutical substance, how the specific heat capacity can be quantitatively calculated from the total heat flow and the heat capacity data of a TMDSC experiment.

2. Experimental

The DSC experiments have been performed using a Mettler Toledo DSC821e, operated by the STARe package, including the temperature-modulated DSC software option (ADSC). To provide the required cooling rates, an intracooler was used as the cooling system. The temperature program of a TMDSC experiment superimposes a conventional linear temperature program onto a small periodical temperature perturbation, i.e.

$$T(t) = T_0 + \beta_0 t + T_a \sin\left(\frac{2\pi t}{t_p}\right) \quad (1)$$

For our experiments, an underlying heating rate (β_0) of 1 K/min, a temperature amplitude (T_a) of 0.5 K, a period (t_p) of 48 s and an initial temperature (T_0) of 5°C were used. The corresponding heat flow signal then reads as

$$\Phi(t) = \Phi_u(t) + \frac{2\pi T_a mc}{t_p}\cos\left(\frac{2\pi t}{t_p} - \varphi\right) \quad (2)$$

Here, Φ_u denotes the total heat flow (similar to the conventional DSC measurements); m, the sample mass; c, the specific heat capacity of the sample; and φ, the phase shift.

The temperature of the DSC821e was calibrated using indium and zinc. The modulated heat flow (Φ_m) of a sample showing a change in the specific heat capacity only can be described by

$$\begin{aligned}\Phi_m &= m \cdot c_p \cdot \frac{dT}{dt} \\ &= K_c \cdot m \cdot c_p\left(T_a \cdot \frac{2\pi}{t_p} \cdot \cos\left(\frac{2\pi}{t_p} \cdot t - \varphi - \varphi_c\right) + \beta_0\right)\end{aligned} \quad (3)$$

Here K_c and φ_c denote the temperature and frequency-dependent calibration functions for the heat flow amplitude and the phase shift, respectively; m is the sample mass; and c_p its specific heat capacity. The calibration functions have been determined by using an aluminum sample analyzed using the temperature program described before. The specific heat capacity of aluminium is well known. Thus, K_c can be calculated using the measured heat flow amplitude for the aluminum sample. Due to its excellent heat conductivity and thermal inertness, the phase shift φ for an aluminum sample is zero. Therefore, the phase shift calibration function φ_c, corresponds to the measured phase shift.

The sample used was a spray-dried mixture of two incompatible amorphous pharmaceutical compounds with a remnant moisture content of about 8%. The samples were run in aluminum pans that were either hermetically-sealed, open or covered with pierced lids, the sample mass being typically 5 mg. The pierced lids used were commercially-available lids with a hole diameter of 50 μm.

3. Results

In Fig. 1 results of conventional DSC measurements are shown for various pan/lid configurations (heating rate 10 K/min). In the open pan, a broad evaporation peak beginning at about 10°C is observed. Peak integration of the baseline-corrected curve c (using curve a as baseline) delivers an endothermal enthalpy change of about 1214 J. In Fig. 2 we show the result of a thermogravimetric analysis. The data show a weight loss of about 8.4% between ambient temperature and 150°C. The mass of the sample used for the DSC experiment in the open pan was 5.652 mg. Thus, the enthalpy change normalized to the weight loss amounts to 2557 J/g, which is in good agreement with the heat of evaporation of water. We conclude that the water loss is akin to that from a free water surface, i.e. the interaction with the substrate is negligible. Strictly speaking, this is only true for the initial constant rate period of the drying process, when the rate-limiting step is the evaporation from the powder bed. At lower water contents, diffusion of water to the surface becomes the rate-limiting step. In this case, the rate and energetics of the evaporation process are no longer equivalent to the free water surface assumption. However, it has to be noted that the details of the evaporation energetics and kinetics do not affect the general methodology outlined in this work.

In our case the normalized enthalpy change amounts to 2557 J/g, which is slightly higher than the heat of evaporation of free water. This indicates that the water is either weakly chemically or physically bonded to the sample, and/or that transportation mechanism has a certain influence on the energetics of the evaporation process. Again, this does not invalidate our model.

The DSC-trace for the hermetically-sealed pan shows several endothermic peaks that cannot be conclusively interpreted. The steep heat flow increase above about 140°C is due to the rapid moisture release when the pressurized pan bursts. In the case of the pierced lid, the evaporation process is shifted to temperatures close to the boiling point of the volatile components. Again, an endothermic peak is observed at about the same temperature as in the run with the hermetically-sealed pan. The curves measured using the hermetically-sealed pan and the pan with the pierced lid both show a distinct peak at around

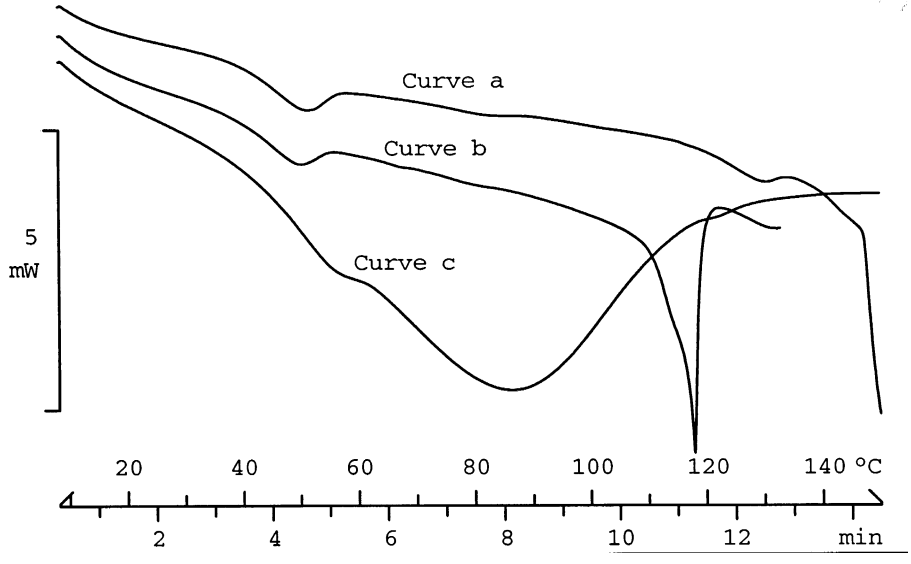

Fig. 1. DSC-measurements of a moist spray-dried pharmaceutical under various pan/lid combinations (curve a: hermetically-sealed pan; curve b: pan with pierced lid (50 μm); curve c: open pan). Sample mass around 5 mg, heating rate 10 K/min.

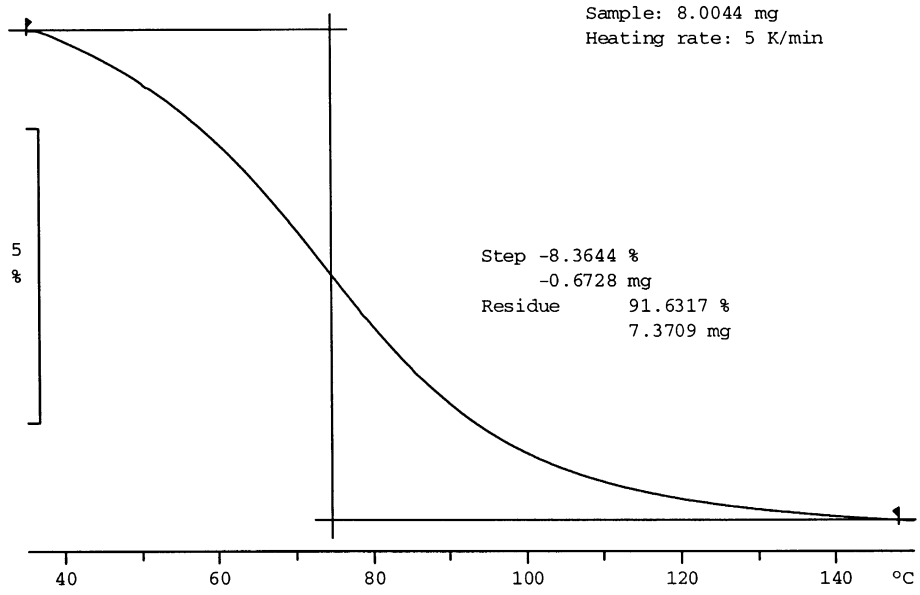

Fig. 2. Thermogravimetric analysis of a moist spray-dried pharmaceutical. Sample mass 8.0044 mg, heating rate 5 K/min.

50°C, due to enthalpy relaxation during the glass transition. Since the moisture content in the open pan measurement is slightly lower due to ongoing evaporation, the glass transition, and also the enthalpy relaxation peak, is shifted to a higher temperature.

Results of the TMDSC measurements are shown in Fig. 3. The temperature axis is the underlying temperature $T_u = T_0 + \beta_0 t$. The samples were run in the open pan and in the pan with a pierced lid (hole diameter 50 μm), respectively. As expected the traces for the total heat flow are similar to the curves shown in Fig. 1. However, since a much lower mean heating rate has been used, the enthalpy relaxation peak and the evaporation peak are shifted. In the case of the open pan, enthalpy relaxation can no longer be clearly identified, and evaporation peaks at around 53°C. In the case of the 50 μm pierced lid, the enthalpy relaxation peak is shifted to about 54°C, and an evaporation peak shows up at around 90°C. Inspection of the specific heat capacity shows quite different behavior between the two samples. In the case of the sample run in the pan with the 50 μm pierced lid, we find a first glass transition at around 55°C. Measuring glass transitions by DSC usually delivers a superposition of the step-like heat capacity change and the enthalpy relaxation peak. In the TMDSC experiment the specific heat capacity does not show such a relaxation peak. As already mentioned, it shows up as the small peak around 54°C in the total heat flow. Another glass transition can be identified at about 132°C. In between, the heat capacity decreases slightly due to the release of moisture.

Due to evaporation, the specific heat capacity of the sample measured in the open pan decreases between 40°C and 80°C. Subsequently, glass transitions at 107°C and 137°C can be seen. The results show that the water acts as a plastiziser for the sample: the glass transition at 54°C corresponds to the moist sample (moisture content of about 5.3%); the glass transition, at about 107°C, to the dry sample.

The glass transitions at 137°C (open pan) and 132°C (pierced lid) are due to the second amorphous compound in the original sample. The temperature difference of this second glass transition can again be explained by the fact that in case of the pierced lid pan, the sample is still slightly moist at 132°C; moisture thus acts as a plastiziser for this second compound also. Using the results

described later, the remnant moisture at 132°C in the pierced lid pan amounts to about 0.65% (c.f. Fig. 6, curve c).

4. Quantitative determination of the specific heat

The heat flow into a sample, Φ, containing some remnant moisture, can be described by

$$\Phi = c_v m_v \beta + c_s m_s \beta + \frac{dm_v}{dt} \cdot \Delta h_e + \xi \quad (4)$$

where c_v and c_s denote the specific heat capacity of the volatile and the effective sample; m_v is the mass of the volatile compounds; m_s the mass of the dried sample; β the heating rate, Δh_e the specific heat of evaporation; and ξ includes any other thermal events apart from evaporation and changes of the specific heat. Usually the heat flow variations due to changes of the specific heats or other thermal events are negligible compared to the contribution due to evaporation processes. Furthermore, if ξ delivers only weak signals (e.g. during glass transitions) Eq. (1) reduces to

$$\Phi \approx \frac{dm_v}{dt} \cdot \Delta h_e + \Phi_b(t) \quad (5)$$

where Φ_b describes the baseline of the evaporation peak.

The remaining amount of the evaporating compound, Φ_{peak}, can be estimated at any given time from a baseline-corrected DSC-trace:

$$\Phi_{peak} = \Phi - \Phi_b = \frac{dm_v}{dt} \cdot \Delta h_e \quad (6)$$

The total area of the evaporation peak delivers the total moisture content. The total amount of the lost volatiles at a certain time, $m_v(t)$, is given by the partial area below the evaporation peak:

$$m_v(t) = \frac{1}{\Delta h_e} \int_{t_0}^{t} \Phi_{peak}\, dt \quad (7)$$

where t_0 denotes the beginning of the evaporation peak.

This procedure is illustrated in Fig. 4. It shows the total heat flow, Φ, as measured in an open pan (curve a). The baseline, Φ_b (curve b), and the baseline-corrected heat flow curve, Φ_{peak}, is displayed as curve c. Curve d, finally, shows the amount of moisture, m_v, still present in the sample as a function of time.

The TMDSC experiment delivers an apparent heat capacity c_a as shown in Fig. 5, curve a. The

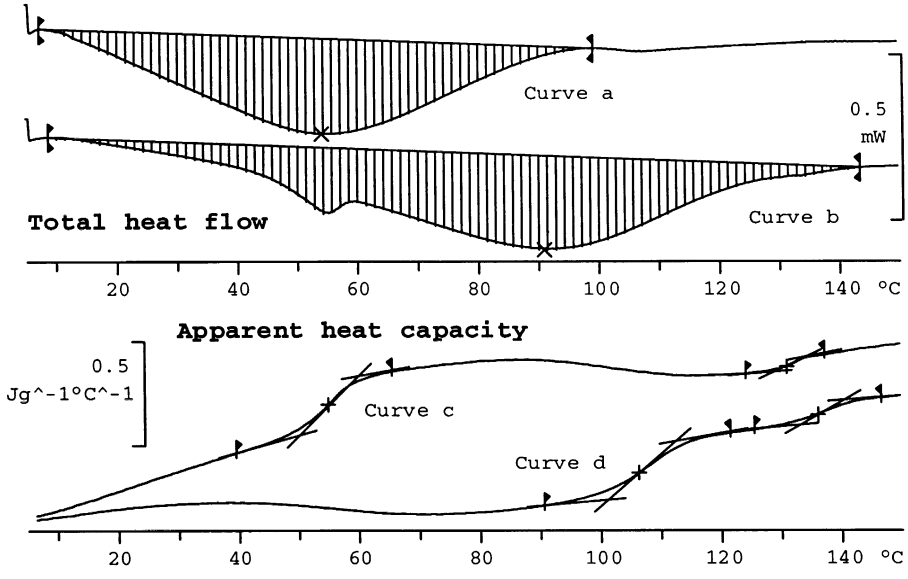

Fig. 3. Total heat flow and apparent heat capacity resulting from an TMDSC experiment for an open pan (curves a and d) and a 50 μm pierced lid pan (curves b and c), respectively. Underlying heating rate 1 K/min.

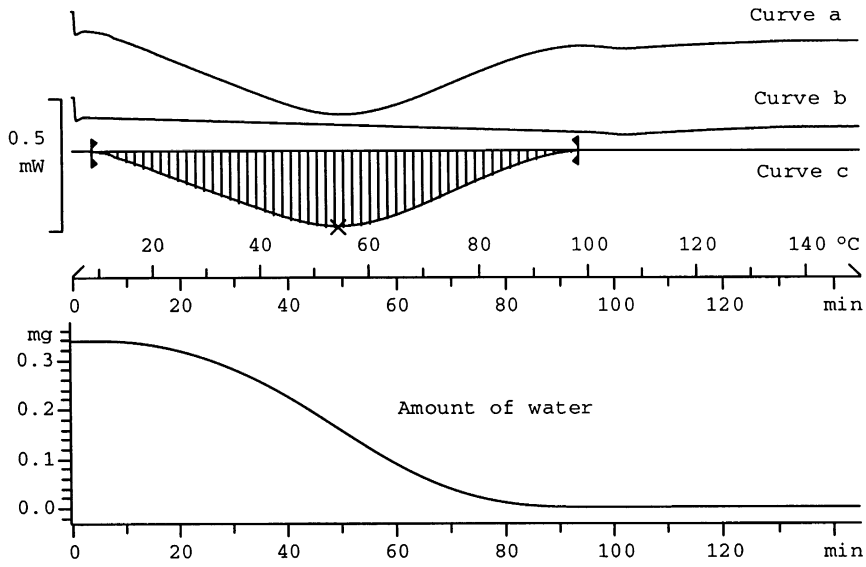

Fig. 4. Estimation of the amount of moisture remaining in the sample as a function of time (curve a: total heat flow, curve b: baseline; curve c: baseline corrected total heat flow).

apparent heat capacity is normalized to the initial sample mass $m_i = m_s + m_v(t=0)$, where m_s denotes the mass of the dried sample. However, this apparent heat capacity has to be corrected for the heat capacity "loss" due to the release of moisture.

This contribution can be determined using the result shown in Fig. 4. The specific heat capacity of the dried sample material, c_s, then amounts to

$$c_s = \frac{m_i}{m_s} \cdot c_a - \frac{m_v(t)}{m_s} \cdot c_v \quad (8)$$

The result, together with the heat capacity contribution of the evolved moisture, is also shown in Fig. 5 (curve b and c, respectively). The c_s-curve increases smoothly and is not affected by the evaporation effect. Using this evaluation procedure, minor thermal effects such as glass transitions are clearly recognized and can be evaluated with better accuracy with respect to its transition temperature and the step height of the heat capacity change. Additionally, these parameters can be correlated to the actual moisture content.

The same procedure has also been applied to measurement in the case of the pierced lid. The results are summarized in Fig. 6. As already mentioned, an enthalpy relaxation peak is observed around 54°C. To estimate the total amount of water, the total heat flow curve has to be corrected for this peak as well as for the baseline. From the net water evaporation peak, one can conclude the amount of water still present in the sample and correct the apparent specific heat capacity for the evolved moisture. As a result, we again get the temperature dependence of the specific heat capacity of the dry sample. Note that at the temperature of the second glass transition (132°C), which was attributed to a second glassy compound in the sample, there is still some moisture left in the sample (0.65%). This explains the temperature difference in T_g of the dry sample measured in the open pan (c.f. Fig. 5) and the sample measured in the pierced lid pan. Comparison with Fig. 5 shows that the initial and the final values of the apparent heat capacity, as well as for the corrected heat capacity, agree for the two measurements. This confirms the fact that at the beginning and at the end of the respective runs, the moisture content is the same, independent of the experimental conditions.

The results of the evaluation of the first glass transition for the sample run in the open pan and

the pierced lid pan are summarized in Table 1. It shows that for the open pan, the step height and the glass transition temperature are not significantly affected by the correction. This is due to the fact that at T_g the remnant moisture is already completely evaporated. The advantage of the correction procedure in this case lies in the fact that the tangent for the glass transition can be determined much more reliably for the corrected than for the uncorrected curve. In case of the pierced lid pan, the step height of the glass transition can only be evaluated correctly if the corrected heat capacity curve is used. As expected, the step height in this case agrees with the glass transition step height as measured for the sample run in the open pan.

5. Conclusion

Temperature modulated DSC is a powerful tool for quantitative measurement of the specific heat of moist samples. From the total heat flow, the amount of the volatile compound can be estimated at any time during the experiment and the apparent specific heat capacity delivers information on thermal processes which are masked by the evaporation peak in conventional DSC. In the presented case, TMDSC is used to investigate the dependence of the glass transition on moisture by simply working with differently-sealed pans. In the present case, we found that a water content of 6.2% shifts the glass transition from about 107°C to about 53°C. Furthermore, the apparent specific heat capacity can be corrected for the volatile component still present in the sample. This delivers the specific heat capacity of the dried sample. In the case of semi crystalline samples, the combination of the outlined correction and the method discussed by Guinot & Leveiller (1999) could be used to estimate the sample crystallinity.

Acknowledgements

The authors would like to thank the referee for his inspiring comments and helpful suggestions.

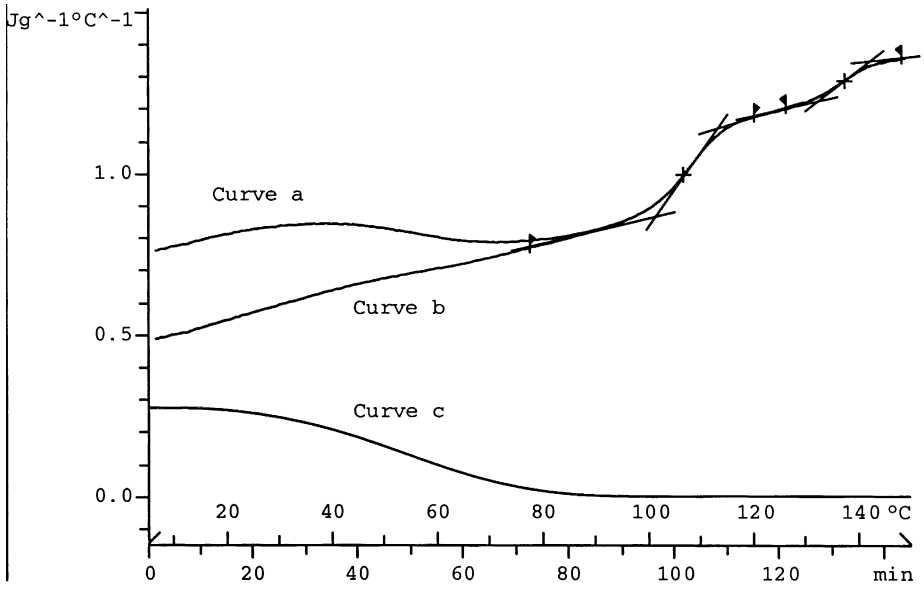

Fig. 5. Correction of the apparent heat capacity by the heat capacity contribution due to the loss of moisture (curve a: apparent heat capacity; curve b: apparent heat capacity, corrected by the amount of evaporated water (curve c)).

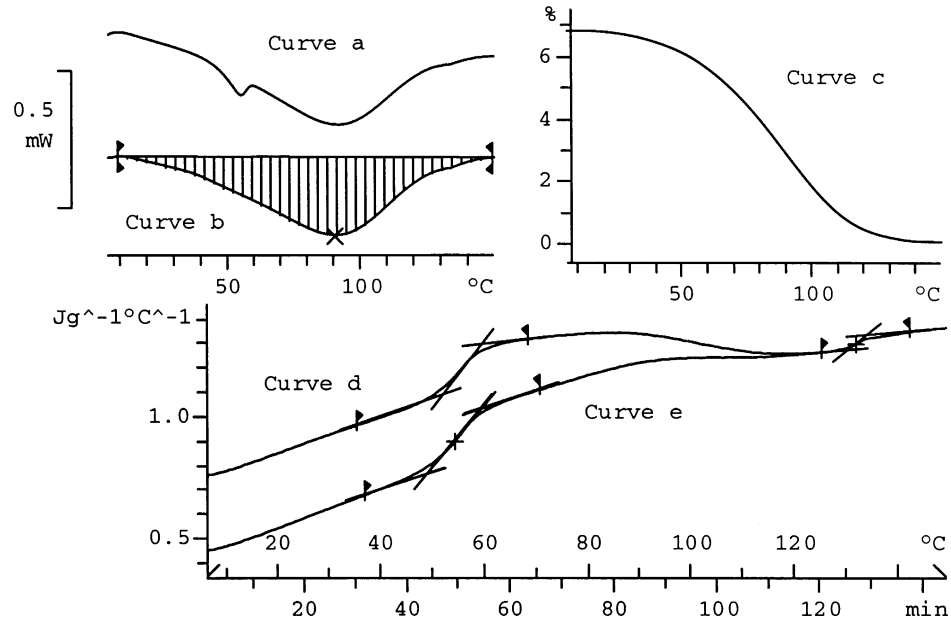

Fig. 6. Evaluation of the specific heat of a pharmaceutical sample run in a pan with a pierced lid. Curve a: original total heat flow; curve b: baseline corrected heat flow; curve c: remnant water content in the sample; curve d: apparent specific heat; curve e: specific heat of the dry sample.

Table 1
Glass transition for the sample run in the open pan and the pierced lid pan before and after correction.

	without correction		with correction		
	T_g in °C	Δc_p in J/(gK)	T_g in °C	Δc_p in J/(gK)	m_v/m_s at T_g
open pan	106	0.25	107	0.26	0.000
pierced lid	55	0.21	54	0.26	0.065

References

Alig, I., Jenninger, W., Schawe, J.E.K., 1998. Temperature modulated differential scanning calorimetry during isothermal curing of phase separating polymer networks. J. Non-Cryst. Solids 235/237, 504-509.

Cassettari, M., Salvetti, G., Tombari, E., Veronesi, S., Johari, G.P., 1992. Thermodynamics of isothermal vitrification by chemical reactions in a liquid. Il Nuovo Cim. 14D, 763–766.

Cheng, Y.Y., Brillhart, M.V., Cebe, P., 1997. Modulated differential scanning calorimetry study of blends of poly(-butylene terephthalate) with polycarbonate. Thermochim. Acta 304/305, 369–378.

Guinot, S., Leveiller, F., 1999. The use of MTDSC to assess the amorphous phase content of a micronised drug substance. Int. J. Pharm. 192, 63–75.

Hill, V.L., Craig, D.Q.M., Feely, L.C., 1998. Characterization of spray-dried lactose using modulated differential scanning calorimetry. Int. J. Pharm. 161, 95–107.

Jin, Y., Bonilla, J., Lin, Y.-G., Morgan, J., MyCracken, L., Carnahan, J., 1996. A study of PBT/PC blends by modulated DSC and conventional DSC. J. Thermal. Anal. 64, 1047–1059.

Monserrat, S., Cima, I., 1999. Isothermal curing of an epoxy resin by alternating differential scanning calorimetry. Thermochim. Acta 330, 189–200.

Reading, M., 1993. Modulated differential scanning calorimetry – a new way forward in materials characterization. Trends Polym. Sci. 1, 248–253.

Riesen, R., Widmann, G., Truttmann, R., 1996. Alternating thermal analysis techniques. Thermochim. Acta 272, 27–39.

Royall, P.G., Craig, D.Q.M., Doherty, C., 1999. Characterization of moister uptake effects on the glass transitional

behavior of an amorphous drug using modulated temperature DSC. Int. J. Pharm. 192, 39–46.

Schawe, J.E.K., Höhne, G.W.H., 1996. Modulated temperature DSC measurements relating to the cold crystallization process of poly(ethylene terephthatate). J. Thermal. Anal. 64, 893–903.

Schick, C., Stoll, B., Schawe, J.E.K., Roger, A., Gnoth, M., 1991. Dielectric and thermal relaxations in low molecular mass liquid crystals. Progr. Colloid Polym. Sci. 85, 148–156.

Sichina, W.J., 1994. Oscillating DSC (ODSC) as problem solving tool. In: Proceedings of the 23rd NATAS Conference, pp. 38–44.

Swier, S., Van Mele, B., 1999. Reaction-induced phase separation in polyethersulfone-modified epoxy-amine systems by temperature modulated differential scanning calorimetry. Thermochim. Acta 330, 175–187.

Toda, A., Oda, T., Hikosaka, M., Saruyama, Y., 1997. A new analyzing of temperature modulated DSC of exo- or endothermic processes: application to polyethylene crystallization. Thermochim. Acta 293, 47–63.

Van Assche, G., Van Hemelrijck, A., Rahier, H., Van Mele, B., 1997. Modulated temperature differential calorimetry: cure, vitrification, and devitrification of thermosetting systems. Thermochim. Acta 304/305, 317–334.